



LIBRARY
ROYAL AIR FORCE ATTACHMENT
BEDFORD.

PROCUREMENT EXECUTIVE, MINISTRY OF DEFENCE

AERONAUTICAL RESEARCH COUNCIL
REPORTS AND MEMORANDA

On the Elastic Moduli of Unidirectional Fibre Reinforced Composites

By E. H. MANSFIELD, F.R.S.
Structures Dept., R.A.E., Farnborough

LONDON: HER MAJESTY'S STATIONERY OFFICE

1976

£2.30 NET

On the Elastic Moduli of Unidirectional Fibre Reinforced Composites

By E. H. MANSFIELD, F.R.S.

Structures Dept., R.A.E., Farnborough

*Reports and Memoranda No. 3782**

July, 1974

Summary

A simple analytical technique is presented for obtaining lower bounds to the effective moduli of unidirectional fibre-reinforced composites with any repetitive array of fibres. The analysis depends upon a direct method involving stress-equilibrium and strain-continuity considerations, and thus it differs from the type of analysis due to Hashin and Hill (and others) involving variational methods. The composite is envisaged as being sliced along all 1,2 planes so that conditions of plane stress exist throughout and the stiffness properties of each vanishingly thin slice are readily determined in terms of the constituent properties of the fibre and matrix. The effective elastic moduli are obtained by suitable integration of such slice properties over a repeating fibre/matrix pattern. Comparison with known accurate values of the longitudinal shear modulus shows that the technique underestimates the modulus by factors of about 1.1 for the square array and 1.2 for the hexagonal array, depending on the fibre volume fraction and fibre/matrix stiffness ratio. By judicious use of such correction factors it should be possible to estimate the longitudinal shear modulus over a wide range of design parameters to within about 5 per cent; for the square and hexagonal arrays Symm's accurate but limited values have been augmented by new results which have an accuracy of 0.3 per cent. New results are also presented for the transverse modulus.

* Replaces R.A.E. Technical Report 74106 — A.R.C. 35 647

LIST OF CONTENTS

1. Introduction
2. Method of Analysis
 - 2.1. The Longitudinal Shear Modulus of Unidirectional FRC
 - 2.2. The Longitudinal and Transverse Moduli of Unidirectional FRC
 - 2.3. Evaluation of $\langle S^*(z) \rangle$
3. Comparisons with Known Solutions
 - 3.1. The Hexagonal Array
 - 3.2. The Square Array
4. Extension of Known Accurate Values for G_{12}^*/G^m
5. The Transverse Modulus Ratio E_2^*/E^m
6. Examples
7. Conclusions

Acknowledgment

List of Symbols

References

Tables 1 to 3

Illustrations — Figures 1 to 7

Detachable Abstract Cards

1. Introduction

Unidirectional fibre-reinforced composite (FRC) may be used in a structural context for carrying unidirectional loads, as in the manner of a strut or reinforcing stringer, or as one of a number of laminates in a built-up sheet for carrying multi-directional loads. In either case there is the problem of load transfer into the member via end fittings. A knowledge of the effective longitudinal, transverse and shear moduli of the member is an essential preliminary to the efficient design of such fittings.

In the multi-laminate sheet it is customary to have at least three distinct alignments for the fibres so that the effective moduli are dominated by the stiffness of the fibres rather than the matrix, and are adequately and simply given by 'netting analysis'.¹ However, in a unidirectional FRC member the transverse and shear moduli are primarily dependent on the stiffness of the matrix rather than the fibre. Theoretical and numerical techniques²⁻⁷ are available for predicting these moduli assuming that the fibres are spaced in regular arrays and a limited number of accurate numerical results for hexagonal and square arrays are given by Symm.⁶ There are also techniques available for deriving upper and lower bounds to the effective moduli for what are called random arrays of fibres.⁸

Here we present a technique for obtaining lower bounds to the effective moduli in unidirectional FRC with *any specified repetitive array*. Comparisons with Symm's accurate results for the longitudinal shear modulus of FRC with hexagonal and square arrays show that the technique under-estimates the true value by about 20 per cent for the hexagonal array and 10 per cent for the square array depending on the fibre volume fraction v_f and the fibre/matrix stiffness ratio. In comparison with Hashin's⁸ 'best lower bound' the present technique is more accurate only at high values of v_f , namely $v_f > 0.85$ for the hexagonal array and $v_f > 0.60$ for the square array. Such an improvement, however limited, is to be expected because Hashin's model requires the presence of fibres with ever-decreasing diameter, which cannot adequately represent a composite with fibres of constant diameter—particularly near the limits of maximum fibre packing. But the main advantages of the present method are (i) its simplicity, (ii) its generality, and (iii) the fact that all known accurate values of the effective moduli are under-estimated by amounts which vary only slightly with v_f and the fibre/matrix stiffness ratio, thus enabling the method to augment the range of accurate results for hexagonal and square arrays. Finally, (iv) the method enables results for the effective longitudinal shear modulus to be used to derive results for the effective transverse modulus of unidirectional FRC.

2. Method of Analysis (see Fig. 1 for notation)

The method of analysis is approximate but simple. It is based on the following closely related facts. First, under an applied longitudinal shear stress τ_{12}^* , the dominant stresses in the matrix and fibre are the longitudinal shear stresses τ_{12}^m and τ_{12}^f in the plane of the applied shear stress: the longitudinal shear stresses in a normal plane, τ_{13}^m and τ_{13}^f , are significantly less. Second, under an applied transverse stress σ_2^* the normal stresses in the matrix and fibre, σ_3^m and σ_3^f are small in comparison with the transverse stresses σ_2^m and σ_2^f .

The present method ignores these normal shear and direct stresses by adopting a *slicing* technique in which the composite is envisaged as being sliced along all 1, 2 planes (like a pack of cards), thus ensuring conditions of plane stress throughout. It is to be noted that this technique introduces an artificial degree of flexibility into the composite so that the resulting values of the composite moduli are *lower limits* to the true values. The degree to which this technique under-estimates the true moduli is determined by comparison with some known exact solutions and appropriate compensating factors are introduced.

The slicing technique greatly simplifies the theoretical determination of the longitudinal shear and transverse moduli of unidirectional FRC with any repetitive array of fibres. In such an FRC the cross-section may be covered by contiguous and equal rectangles containing identical fibre patterns. The sides of the rectangles may cut through individual fibres and the rectangles themselves may be staggered, as shown in Fig. 3. The effective elastic moduli of such an FRC are the same as for the individual strips of rectangular section whose faces are displaced by fixed amounts. The effective elastic moduli of an individual strip are determined by integration (through the height h) of the effective moduli of the constituent slices of width w bounded by vanishingly close planes at $z, z + \delta z$.

The matrix is assumed to be isotropic with shear modulus G^m , Young's modulus E^m and Poisson's ratio ν^m . The fibre material is assumed to have a longitudinal shear modulus G^f and orthotropic direct stiffness characteristics with longitudinal and transverse Young's moduli E_1^f and E_2^f and corresponding Poisson's ratios ν_{21}^f and ν_{12}^f . (For numerical purposes we later take $\nu_{12}^f = \nu^m$ as this considerably simplifies the analysis without significantly affecting results.) Average or effective values of the moduli and stresses for the composite are

denoted by an asterisk. The overall volume fractions are denoted by v_m and v_f ($v_m + v_f = 1$), while the volume fractions appropriate to a slice at z are denoted by $v_m(z)$ and $v_f(z)$. We adopt the notation $\langle f(z) \rangle$ to indicate the average value of $f(z)$ through the height h of the repeating rectangle, i.e.

$$\langle f(z) \rangle = \frac{1}{h} \int_0^h f(z) dz$$

and we note in passing that, for example,

$$\langle v_f(z) \rangle = v_f.$$

Fig. 2 shows average and local stresses in a typical slice.

2.1. The Longitudinal Shear Modulus of Unidirectional FRC

The stress–strain relations in shear for the matrix and fibre material are

$$\left. \begin{aligned} \gamma_{12}^m &= \tau_{12}^m / G^m, \\ \gamma_{12}^f &= \tau_{12}^f / G^f, \end{aligned} \right\} \quad (1)$$

while from equilibrium considerations

$$\tau_{12}^*(z) = \tau_{12}^m(z) = \tau_{12}^f(z). \quad (2)$$

The average shear strain in a typical lamina at z is given by

$$\gamma_{12}^* = v_m(z) \gamma_{12}^m(z) + v_f(z) \gamma_{12}^f(z), \quad (3)$$

and accordingly the effective longitudinal shear modulus is given by

$$\begin{aligned} G_{12}^*(z) &= \tau_{12}^*(z) / \gamma_{12}^* \\ &= \left(\frac{v_m(z)}{G^m} + \frac{v_f(z)}{G^f} \right)^{-1}, \end{aligned} \quad (4)$$

and it is convenient to re-write this in the form

$$\begin{aligned} G_{12}^*(z) / G^m &= S^*(z), \quad \text{say} \\ &= \{1 - (1 - \eta)v_f(z)\}^{-1} \end{aligned} \quad (5)$$

where

$$\eta = G^m / G^f.$$

Finally, by integrating through the height h of the repeating rectangle we obtain

$$G_{12}^* / G^m = \langle S^*(z) \rangle. \quad (6)$$

The above analysis can readily be extended to include an FRC containing fibres with differing moduli. An example is given in Section 6.

2.2. The Longitudinal and Transverse Moduli of Unidirectional FRC

The direct stress–strain relations in the matrix and fibre material are given by

$$\begin{aligned} \epsilon_1^m &= (\sigma_1^m - \nu^m \sigma_2^m) / E^m, \\ \epsilon_2^m &= (\sigma_2^m - \nu^m \sigma_1^m) / E^m, \\ \epsilon_1^f &= \sigma_1^f / E_1^f - \nu_{21}^f \sigma_2^f / E_2^f, \\ \epsilon_2^f &= \sigma_2^f / E_2^f - \nu_{12}^f \sigma_1^f / E_1^f, \end{aligned} \quad (7)$$

where, for example, ν_{12}^f is the ratio (transverse contraction of fibre)/(longitudinal extension) due to a longitudinal stress. For an elastic material—as the fibres are assumed to be—it follows from the Reciprocal Theorem that

$$\nu_{21}^f/E_2^f = \nu_{12}^f/E_1^f. \quad (8)$$

Equilibrium of average direct stresses with component stresses in a typical slice gives

$$\text{and} \quad \left. \begin{aligned} \sigma_1^*(z) &= v_m(z)\sigma_1^m(z) + v_f(z)\sigma_1^f(z) \\ \sigma_2^*(z) &= \sigma_2^m(z) = \sigma_2^f(z), \end{aligned} \right\} \quad (9)$$

while the average direct strains are related to the component strains by

$$\text{and} \quad \left. \begin{aligned} \varepsilon_1^*(z) &= \varepsilon_1^m(z) = \varepsilon_1^f(z) \\ \varepsilon_2^*(z) &= v_m(z)\varepsilon_2^m(z) + v_f(z)\varepsilon_2^f(z). \end{aligned} \right\} \quad (10)$$

Equations (7) to (10) enable us to relate the average direct strains to the average direct stresses in a typical slice:

$$\left. \begin{aligned} \varepsilon_1^*(z) &= \sigma_1^*(z)/E_1^*(z) - \nu_{21}^*(z)\sigma_2^*(z)/E_2^*(z), \\ \varepsilon_2^*(z) &= \sigma_2^*(z)/E_2^*(z) - \nu_{12}^*(z)\sigma_1^*(z)/E_1^*(z), \\ \nu_{21}^*(z)/E_2^*(z) &= \nu_{12}^*(z)/E_1^*(z). \end{aligned} \right\} \quad (11)$$

where

Finally, for the composite as a whole, we are now in a position to relate the average direct strains to the average direct stresses:

$$\left. \begin{aligned} \varepsilon_1^* &= \sigma_1^*/E_1^* - \nu_{21}^*\sigma_2^*/E_2^*, \\ \varepsilon_2^* &= \sigma_2^*/E_2^* - \nu_{12}^*\sigma_1^*/E_1^*, \\ \nu_{21}^*/E_2^* &= \nu_{12}^*/E_1^*. \end{aligned} \right\} \quad (12)$$

where

Now in determining E_1^* and E_2^* it is not, in general, simply a matter of integrating $E_1^*(z)$ and $E_2^*(z)$ through the height h because we must ensure that *both* the average direct strains $\varepsilon_1^*(z)$ and $\varepsilon_2^*(z)$ are the same for all slices. This problem did not arise for the case of shear because $\gamma_{12}^*(z)$ was the only non-zero strain. However, for the modulus E_1^* a simple integration of $E_1^*(z)$ is valid if

$$\nu^m = \nu_{12}^f = \nu, \quad \text{say.} \quad (13)$$

This is because under an applied stress $\sigma_1^*(z)$ the average strains are now such that

$$\varepsilon_2^*(z) = -\nu\varepsilon_1^*(z) \quad (14)$$

so that equality of longitudinal strains in all slices necessarily implies equality of transverse strains and, in particular,

$$\nu_{12}^* = \nu. \quad (15)$$

With this simplifying assumption it may be confirmed that

$$E_1^*(z) = v_m(z)E^m + v_f(z)E_1^f$$

which may legitimately be integrated to recover the well-known result:

$$E_1^* = v_mE^m + v_fE_1^f. \quad (16)$$

The simplest way to derive E_2^* is via the plane strain modulus

$$\bar{E}_2^* = \left(\frac{\sigma_2^*}{\epsilon_2^*} \right)_{\epsilon_1^* = 0}, \quad (17)$$

making use of the relation

$$\bar{E}_2^* = E_2^* / (1 - \nu_{12}^* \nu_{21}^*), \quad (18)$$

which yields

$$E_2^* = \left(\frac{1}{\bar{E}_2^*} + \frac{\nu^2}{E_1^*} \right)^{-1}, \quad (19)$$

in virtue of equation (15) and the last of equation (12).

Now under conditions of plane strain ($\epsilon_1^* = 0$) it may readily be verified that

$$\left. \begin{aligned} \bar{E}_2^*(z) &= \left(\frac{v_m(z)}{\bar{E}^m} + \frac{v_f(z)}{\bar{E}_2^f} \right)^{-1}, \\ \bar{E}^m &= E^m / (1 - \nu^2), \\ \bar{E}_2^f &= E_2^f / (1 - \nu_{12}^f \nu_{21}^f). \end{aligned} \right\} \quad (20)$$

This result has much in common with equation (4) for the shear modulus and it is convenient to express it in like form:

$$\left. \begin{aligned} \bar{E}_2^*(z) / \bar{E}^m &= S^*(z) \\ &= \{1 - (1 - \eta') v_f(z)\}^{-1} \\ \eta' &= \bar{E}^m / \bar{E}_2^f. \end{aligned} \right\} \quad (21)$$

Finally, by integrating through the height h of the repeating rectangle we obtain

$$\bar{E}_2^* / \bar{E}^m = \langle S^*(z) \rangle, \quad (22)$$

which is formally identical to equation (6) apart from the replacement of η by η' .

From a numerical standpoint the determination of G_{12}^* , \bar{E}_2^* , and hence E_2^* , thus requires the evaluation of the same function, namely $\langle S^*(z) \rangle$, but with differing values of the constants η , η' .

2.3. Evaluation of $\langle S^*(z) \rangle$

The numerical value of $\langle S^*(z) \rangle$ for any given FRC array may, of course, be determined from $S^*(z)$ by simple graphical integration. Analytical or computer-programmed integration requires a functional expression for $v_f(z)$ and hence expressions for the chord length $c_n(z)$ of a fibre cross-section cut by a section at z . Such expressions for fibres of circular, but not necessarily equal, cross-section are given below.

The equation for a circle of radius r_n whose centre is at y_n , z_n is given by

$$(y - y_n)^2 + (z - z_n)^2 = r_n^2, \quad (23)$$

and accordingly at a typical section z ,

$$y - y_n = \pm \{r_n^2 - (z - z_n)^2\}^{\frac{1}{2}}$$

and hence

$$c_n(z) = 2\{r_n^2 - (z - z_n)^2\}^{\frac{1}{2}}.$$

Note that this expression, and hence $\langle S^*(z) \rangle$, is independent of the value of y_n ; this is a direct consequence of the inherent approximation involved in the 'slicing technique'. It is also tacitly assumed that $(z - z_n)^2 < r_n^2$, otherwise there is no intersection and $c_n(z)$ is zero. This possibility can be catered for simply by writing

$$c_n(z) = 2\mathcal{R}\{r_n^2 - (z - z_n)^2\}^{\frac{1}{2}}, \quad (24)$$

where \mathcal{R} stands for 'the real part of'.

The width of the repeating rectangular element is w and the volume fraction $v_f(z)$ is thus given by

$$\begin{aligned} v_f(z) &= \frac{1}{w} \sum_n c_n(z) \\ &= \frac{2}{w} \sum_n \mathcal{R}\{r_n^2 - (z - z_n)^2\}^{\frac{1}{2}}, \end{aligned} \quad (25)$$

where the summation extends over all *effective* values of n ; *effective*, because any segments of circles cut by the sides of the rectangle at $y = 0$, w can be combined to form a complete segment for purposes of calculation.

3. Comparisons with Known Solutions

We now turn our attention to comparisons with Symm's⁶ accurate values of G_{12}^*/G^m for hexagonal and square arrays of fibres of equal circular cross-section. In this connection we note that for $v_f < 0.4$ (which is generally outside the practical range of interest) the fibres are sufficiently sparse for the interaction effect between fibres to be so small that the distinction between G_{12}^* for the hexagonal and square arrays is negligible and both are adequately given by Hashin's⁸ simple model and formula:

$$\frac{G_{12}^*}{G^m} = \frac{(1 + v_f) + \eta(1 - v_f)}{(1 - v_f) + \eta(1 + v_f)} \quad (26)$$

3.1. The Hexagonal Array

A suitable rectangular repeating element for the hexagonal array is identified by the corner points $OABC$ in the y, z plane in Fig. 4, where

$$\text{and} \quad \left. \begin{aligned} w &= \text{fibre pitch} \\ h &= \frac{\sqrt{3}}{2} w. \end{aligned} \right\} \quad (27)$$

In terms of the fibre volume fraction v_f the radius r is given by

$$\frac{r}{w} = \left(\frac{\sqrt{3}}{2\pi} v_f \right)^{\frac{1}{2}}. \quad (28)$$

[It is convenient at this point to take $w = 1$, so that r, h, z are expressed as proportions of the fibre pitch.] The circles centred on O and A can be combined to form a single effective circle, as previously described, so that equation (25) becomes

$$v_f(z) = \frac{2}{w} \mathcal{R}[(r^2 - z^2)^{\frac{1}{2}} + \{r^2 - (z - h)^2\}^{\frac{1}{2}}]. \quad (29)$$

When $r \leq \frac{1}{2}h$, which corresponds to the range

$$v_f \leq \frac{\pi\sqrt{3}}{8} = 0.68, \quad (30)$$

no single z -section cuts both upper and lower circles, and the two terms in square brackets in equation (29) do not exist simultaneously. The expression for $v_f(z)$ accordingly splits up into the following simple components:

$$v_f(z) = \left. \begin{aligned} &= \frac{2}{w} (r^2 - z^2)^{\frac{1}{2}}, && \text{over the range } 0 < z < r, \\ &= 0 && \text{over the range } r < z < (h-r), \\ &= \frac{2}{w} \{r^2 - (z-h)^2\}^{\frac{1}{2}} && \text{over the range } (h-r) < z < h. \end{aligned} \right\} \quad (31)$$

The corresponding values of $S^*(z)$, given by equation (5), lend themselves to closed form integration to yield

$$\frac{G_{12}^*}{G^m} = 1 - \frac{2\lambda}{\sqrt{3}} + \frac{1}{(1-\eta)\sqrt{3}} \left\{ -\pi + \frac{4}{\sqrt{(1-\mu^2)}} \tan^{-1} \left(\frac{1+\mu}{1-\mu} \right)^{\frac{1}{2}} \right\},$$

where
$$\lambda = \left(\frac{2\sqrt{3}}{\pi} v_f \right)^{\frac{1}{2}} \quad (32)$$

and
$$\mu = \lambda(1-\eta).$$

For values of v_f greater than that given by equation (30), G_{12}^*/G^m has been obtained by a simple computer program.

The factors K by which the present values of G_{12}^*/G^m must be multiplied to bring them into agreement with Symm's accurate values are shown in Fig. 5. It is seen that K varies with v_f and G^f/G^m in a slight and smooth manner everywhere. The relatively large magnitude of K is a reflection of the fact that the slicing technique, which ignores the shear stresses τ_{13} , cannot adequately represent those lines of shear which, in the hexagonal array, zigzag between adjacent rows of fibres. Markedly smaller values of K are to be expected for the square array where, from symmetry, there are no lines of shear which cross from row to row.

3.2. The Square Array

The analysis for the square array has much in common with that for the hexagonal array and accordingly the details will be omitted. Suffice it to say that the following closed form expression exists for all values of v_f :

$$\frac{G_{12}^*}{G^m} = 1 - \kappa + \frac{1}{(1-\eta)} \left\{ -\frac{\pi}{2} + \frac{2}{\sqrt{(1-\rho^2)}} \tan^{-1} \left(\frac{1+\rho}{1-\rho} \right)^{\frac{1}{2}} \right\},$$

where
$$\kappa = \left(\frac{4}{\pi} v_f \right)^{\frac{1}{2}} \quad (33)$$

and
$$\rho = \kappa(1-\eta).$$

The factors K by which these values must be multiplied to bring them into agreement with Symm's accurate values are shown in Fig. 6.

4. Extension of Known Accurate Values for G_{12}^*/G^m

In this section use is made of the present technique and the smoothly varying nature of the correction factors K to extend Symm's⁶ results, which correspond to the circles in Figs. 5 and 6, to the following additional values of v_f : 0.45, 0.50, 0.60, 0.65, 0.75. The method permits an accuracy of about 0.3 per cent.

While the values of G_{12}^*/G^m given by Symm have been described as accurate, it is only fair to point out, as Symm has done, that the collocation procedure he adopted did not converge for certain values of v_f and G^f/G^m . For the hexagonal array nonconvergence occurred at $v_f = 0.9$ for $G^f/G^m = 120, \infty$, while for the square array nonconvergence occurred at $v_f = 0.78$ for $G^f/G^m = 12, 20, 120, \infty$. The value of G_{12}^*/G^m derived for the last combination cited is clearly in error as it is less (by about 1.1 per cent) than the present lower limit. The other values tend to show irregular variations in the factors K . Because of the resulting uncertainty these values are queried in Table 1 and omitted altogether from Table 2.

5. The Transverse Modulus Ratio E_2^*/E^m

The transverse modulus E_2^* is given by equation (19), in which E_1^* is given by equation (16). Thus we find

$$\frac{E_2^*}{E^m} = \left\{ \frac{1-\nu^2}{(\bar{E}_2^*/\bar{E}^m)} + \frac{\nu^2}{1-\nu_f + \nu_f(E_1^f/E^m)} \right\}^{-1} \quad (34)$$

where a lower limit to \bar{E}_2^* is given by equation (22).

Now we have seen in Section 2.2 that the slicing technique yields a lower limit for the plane strain modulus ratio \bar{E}_2^*/\bar{E}^m which is formally identical to equation (6) for the longitudinal shear modulus ratio G_{12}^*/G^m . Accurate values for G_{12}^*/G^m are also known and it is tempting to assume that, for given values of η , η' , the lower limits for G_{12}^*/G^m and \bar{E}_2^*/\bar{E}^m under-estimate the true values by the same amounts. With this assumption we can use Table 1 to determine 'corrected' values of \bar{E}_2^*/\bar{E}^m and hence (presumably) more accurate values for E_2^*/E^m . This has been done in Table 3 for the hexagonal array, making the further assumption that

$$\nu = 0.25, \quad (35)$$

and

$$E_1^f/E^m = \bar{E}_2^f/\bar{E}^m, \quad (36)$$

so that the fibres are effectively isotropic. For the particular case in which $E_2^f/E^m = 20$, Chen and Cheng³ obtained numerical results for the hexagonal array which are based on a classical elasticity solution. Their derived variation of E_2^* with ν_f is in excellent agreement with values obtained from Table 3, although their graphical method of presentation does not permit much accuracy.

As for the influence of fibre anisotropy, it is clear that the transverse modulus of FRC depends more on the transverse modulus of the fibres E_2^f than on the more readily measured longitudinal modulus E_1^f . The use of Table 3 requires a knowledge of E_2^f (or more precisely \bar{E}_2^f/\bar{E}^m) and the derived values of E_2^* differ little from those appropriate to anisotropic fibres with values of E_1^f which do not satisfy equation (36). An example is considered in Section 6.

6. Examples

The following examples illustrate accurate methods of interpolation in the tables of elastic moduli ratios, the influence of fibre anisotropy and the use of the slicing technique to investigate an FRC containing two different types of fibre.

(1) Determine G_{12}^*/G^m for an FRC in which $\nu_f = 0.65$ and $G^f/G^m (= 1/\eta) = 50$.

Equation (26) suggests that the following group of terms

$$\left\{ \left(\frac{1-\nu_f}{1+\nu_f} \right) + \eta \right\} \frac{G_{12}^*}{G^m},$$

hereafter denoted by $\Phi(\eta)$, will vary smoothly with η . A simple calculation from Table 1 shows that as η assumes successive values of 1/6, 1/12, 1/20, 1/120, 0, the function $\Phi(\eta)$ equals 1.038, 1.024, 1.020, 1.014, 1.014 respectively. A plot of $\Phi(\eta)$ against η indicates that $\Phi(1/50) \approx 1.016$, and hence

$$\begin{aligned} \frac{G_{12}^*}{G^m} &= \frac{1.016}{\left(\frac{1-\nu_f}{1+\nu_f} \right) + \frac{1}{50}} \\ &= 4.38. \end{aligned}$$

(2) Determine the influence of fibre anisotropy on the transverse modulus of an FRC in which

$$\nu_f = 0.65, \quad \bar{E}_2^f/\bar{E}^m = 20, \quad \nu = 0.25.$$

If $E_1^f/E^m = \bar{E}_2^f/\bar{E}^m$ the transverse modulus is given by Table 3:

$$E_2^*/E^m = 4.07.$$

However, if $E_1^f/E^m = k\bar{E}_2^f/\bar{E}^m$, say, where k is a measure of the fibre anisotropy, it may be shown from equation (34) that as k increases from 1 to ∞ the ratio E_2^*/E^m increases from 4.07 to 4.14, an increase of less than 2 per cent.

(3)^a Determine G_{12}^*/G^m for an FRC containing fibres with differing moduli and volume fractions, identified by suffices 1 and 2, specified by

$$v_m = 0.35 \quad (\text{so that } v_{f1} + v_{f2} = 0.65),$$

$$v_{f1} = \frac{1}{3}v_{f2},$$

$$G^{f1}/G^m = 6$$

and

$$G^{f2}/G^m = 50.$$

The fibres are of the same size and in an hexagonal array as shown in Fig. 7.

Application of the slicing technique over the repeating rectangle shown dotted in Fig. 7 shows that over the range $0 < z < \frac{1}{2}h$ the FRC has a longitudinal shear modulus appropriate to that determined in example (1):

$$[G_{12}^*/G^m]_{0 < z < \frac{1}{2}h} = 4.38. \quad (37)$$

Over the range $\frac{1}{2}h < z < h$, equation (4) becomes

$$\left. \begin{aligned} G_{12}^*(z) &= \left(\frac{v_m(z)}{G^m} + \frac{v_{f1}(z)}{G^{f1}} + \frac{v_{f2}(z)}{G^{f2}} \right)^{-1} \\ &= \left\{ \frac{v_m(z)}{G^m} + \frac{1}{2}\{1 - v_m(z)\} \left(\frac{1}{G^{f1}} + \frac{1}{G^{f2}} \right) \right\}^{-1} \\ &= \left(\frac{v_m(z)}{G^m} + \frac{\{1 - v_m(z)\}}{G_{\text{eff}}^f} \right)^{-1} \end{aligned} \right\} \quad (38)$$

where G_{eff}^f is the *harmonic mean* of G^{f1} and G^{f2} , i.e.

$$\begin{aligned} \frac{G_{\text{eff}}^f}{G^m} &= \frac{1}{2} \left(\frac{1}{6} + \frac{1}{50} \right)^{-1} \\ &= 10.72. \end{aligned} \quad (39)$$

Applying the interpolation technique of example (1) gives

$$\Phi(1/10.72) \approx 1.025$$

and hence,

$$[G_{12}^*/G^m]_{\frac{1}{2}h < z < h} = 3.36. \quad (40)$$

Finally, according to the slicing technique the overall value of G_{12}^*/G^m is the *arithmetic mean* of equations (37) and (40):

$$G_{12}^*/G^m = 3.87. \quad (41)$$

This value is some 10 per cent less than that obtained by representing the FRC by one with fibres of equal stiffness calculated on a simple 'rule of mixtures' in which $G^f/G^m = 39$.

7. Conclusions

A simple analytical technique has been presented for obtaining lower bounds to the effective elastic moduli of unidirectional fibre reinforced composite (FRC) with any repetitive array of fibres. The unidirectional FRC is envisaged as being sliced along all 1,2 planes so that conditions of plane stress exist throughout and the stiffness properties of each vanishingly thin slice are readily determined in terms of the constituent properties of the fibre and matrix. The effective elastic moduli of the unidirectional FRC are obtained by suitable integration of such slice properties over a repeating fibre/matrix pattern. The lower bound for the transverse modulus is shown to depend on a similar function of the section properties as does the longitudinal shear modulus. Comparison with known accurate values of the longitudinal shear modulus shows that the technique under-estimates the modulus by factors of about 1.1 for the square array and 1.2 for the hexagonal array, depending on the fibre volume fraction and fibre/matrix stiffness ratio. By judicious use of such correction factors it should be possible to estimate the longitudinal shear modulus over a wide range of design parameters to within about 5 per cent; for the square and hexagonal arrays Symm's accurate but limited values have been augmented by new results which have an accuracy of 0.3 per cent. New results are also presented for the transverse modulus.

Acknowledgment

The author is grateful to Miss Doreen Best for the computation.

LIST OF SYMBOLS

$c_n(z)$	Chord length of fibre cut by section at z
E	Young's modulus
\bar{E}	Plane strain modulus, <i>see</i> equations (17), (20)
G	Shear modulus
h	Height of repeating rectangle in fibre array
K	Correction factors for longitudinal shear modulus
r_n	Radius of n th fibre
$S^*(z)$	Defined by equation (5) or (21)
v	Volume fraction
w	Width of repeating rectangle in fibre array
x, y, z	Cartesian coordinates, $0x$ in fibre direction, $0y, 0z$ parallel to w, h
y_n, z_n	Coordinates of centre of n th fibre of circular section
γ	Shear strain
ε	Direct strain
$\Phi(\eta)$	Introduced in Section 6
η, η'	$G^m/G^f, \bar{E}^m/\bar{E}_2^f$ respectively
ν	Poisson's ratio
σ	Direct stress
τ	Shear stress
$\langle \dots \rangle$	$\frac{1}{h} \int_0^h \dots dz$

Suffices or indices m, f refer to matrix or fibre

Suffices 1, 2, 3 refer to cartesian axes x, y, z respectively

Asterisk * refers to average or effective values

REFERENCES

- | <i>No.</i> | <i>Author(s)</i> | <i>Title, etc.</i> |
|------------|---------------------------------|--|
| 1 | H. L. Cox | Elasticity and strength of paper and other fibrous materials.
<i>Brit. J. Appl. Phys.</i> , 3 , 72 (1952) |
| 2 | C. H. Chen | Fibre-reinforced composites under longitudinal shear loading.
<i>J. Appl. Mech.</i> , 37 , 198 (1970). |
| 3 | C. H. Chen and S. Cheng | Mechanical properties of fibre-reinforced composites.
<i>J. Composite Materials</i> , 1 , 30 (1967). |
| 4 | M. D. Heaton | A calculation of the elastic constants of a unidirectional fibre-reinforced composite.
<i>Brit. J. Appl. Phys. Ser 2</i> , 1 , 1039 (1968). |
| 5 | G. Pickett | Elastic moduli of fibre-reinforced plastic composites in:
<i>Fundamental aspects of fibre-reinforced plastic composites.</i>
(Schwartz & Schwartz, eds.) Interscience Publishers, New York (1968). |
| 6 | G. T. Symm | The longitudinal shear modulus of a unidirectional fibrous composite.
<i>J. Composite Materials</i> , 4 , 426 (1970) |
| 7 | G. P. Sendeckyj | Longitudinal shear deformation of composites—effective shear modulus.
<i>J. Composite Materials</i> , 4 , 500 (1970). |
| 8 | Z. Hashin and B. W. Rosen | The elastic moduli of fibre-reinforced materials.
<i>J. Appl. Mech.</i> , 31 , 223 (1964). |

TABLE 1
Values of G_{12}^*/G^m for Hexagonal Array

v_f	$G^f/G^m = 6$	12	20	120	∞
0.40	1.80	2.02	2.14	2.30	2.33
0.45	1.95	2.23	2.37	2.59	2.64
0.50	2.11	2.47	2.65	2.94	3.00
0.55	2.30	2.75	2.99	3.37	3.46
0.60	2.50	3.08	3.39	3.91	4.03
0.65	2.74	3.47	3.89	4.61	4.78
0.70	3.02	3.95	4.53	5.55	5.81
0.75	3.34	4.57	5.38	6.93	7.35
0.80	3.73	5.39	6.60	9.18	9.96
0.85	4.22	6.58	8.54	13.70	15.70
0.90	4.87	8.63	12.80	35.3?	56.2?

TABLE 2
Values of G_{12}^*/G^m for Square Array

v_f	$G^f/G^m = 6$	12	20	120	∞
0.40	1.81	2.03	2.15	2.31	2.35
0.45	1.96	2.24	2.39	2.62	2.67
0.50	2.13	2.50	2.70	3.00	3.08
0.55	2.33	2.81	3.08	3.51	3.61
0.60	2.56	3.19	3.56	4.19	4.35
0.65	2.83	3.69	4.23	5.20	5.46
0.70	3.17	4.38	5.21	6.93	7.43
0.75	3.62	5.47	7.00	11.20	12.80

TABLE 3
Values of E_2^*/E^m for Hexagonal Array ($\nu = 0.25$)

v_f	$\bar{E}_2^f/\bar{E}^m = 6$	12	20	120	∞
0.40	1.84	2.10	2.25	2.45	2.49
0.45	2.00	2.32	2.49	2.76	2.82
0.50	2.16	2.57	2.78	3.12	3.20
0.55	2.35	2.86	3.13	3.58	3.69
0.60	2.56	3.20	3.55	4.15	4.30
0.65	2.80	3.60	4.07	4.90	5.10
0.70	3.09	4.08	4.73	5.88	6.20
0.75	3.40	4.71	5.62	7.36	7.84
0.80	3.80	5.56	6.85	9.71	10.60
0.85	4.27	6.73	8.77	14.50	16.80
0.90	4.90	8.75	13.00	36.9?	60.0?

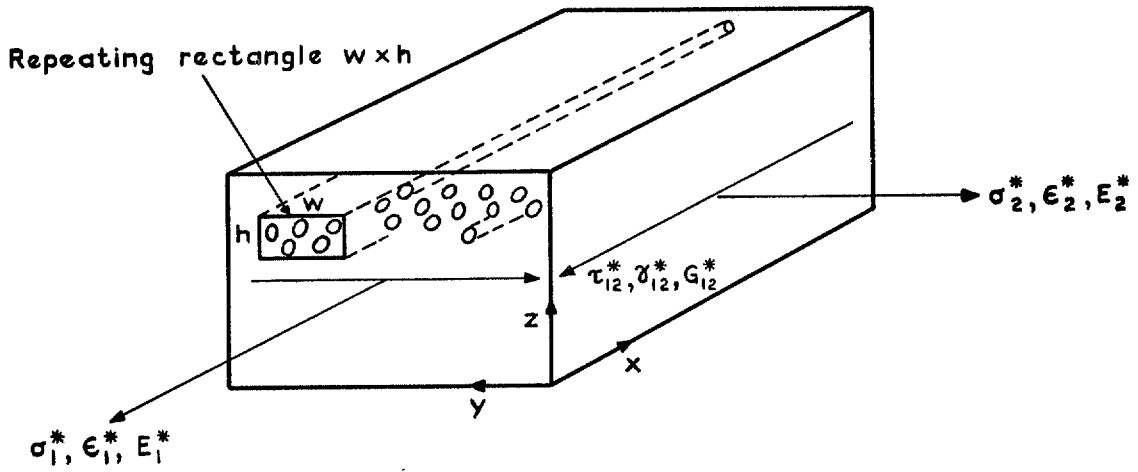


FIG. 1. Diagram showing notation

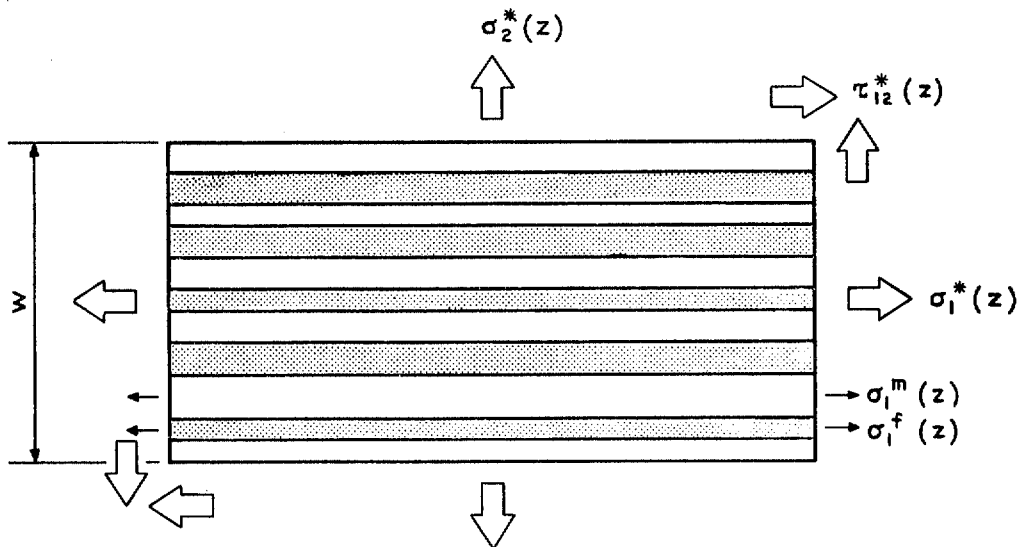


FIG. 2. Stresses acting on thin slice

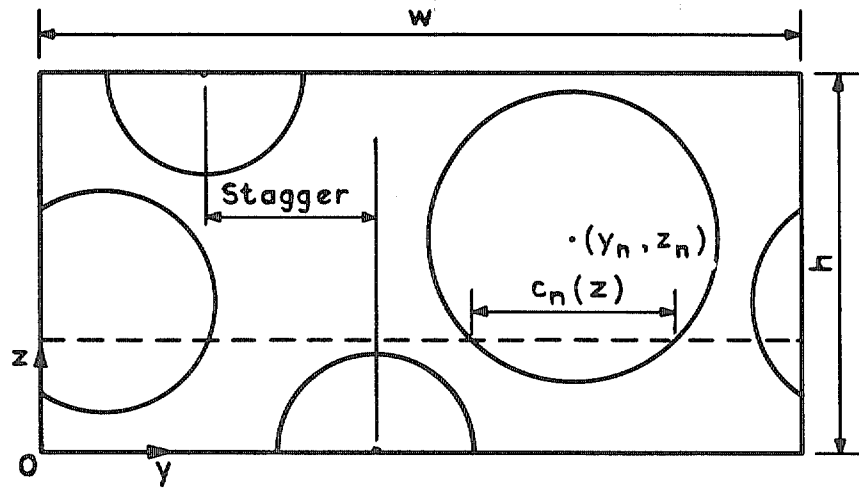


FIG. 3. General repeating rectangle

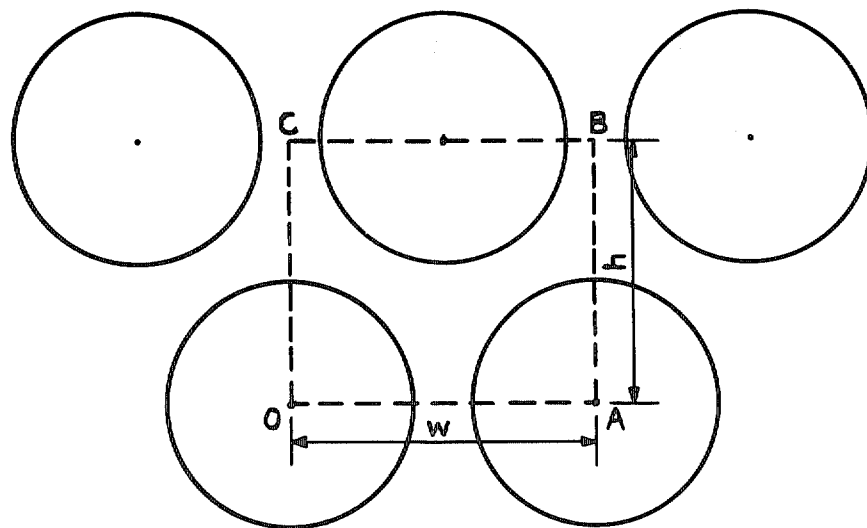


FIG. 4. Repeating rectangle for hexagonal array

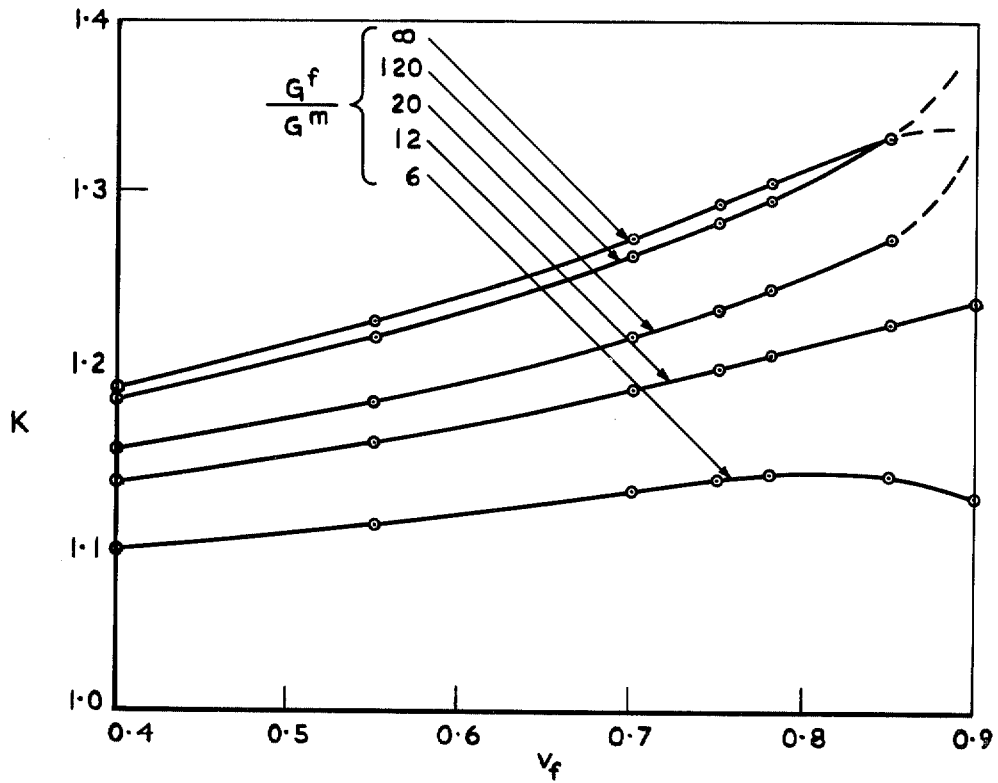


FIG. 5. Correction factors for hexagonal array

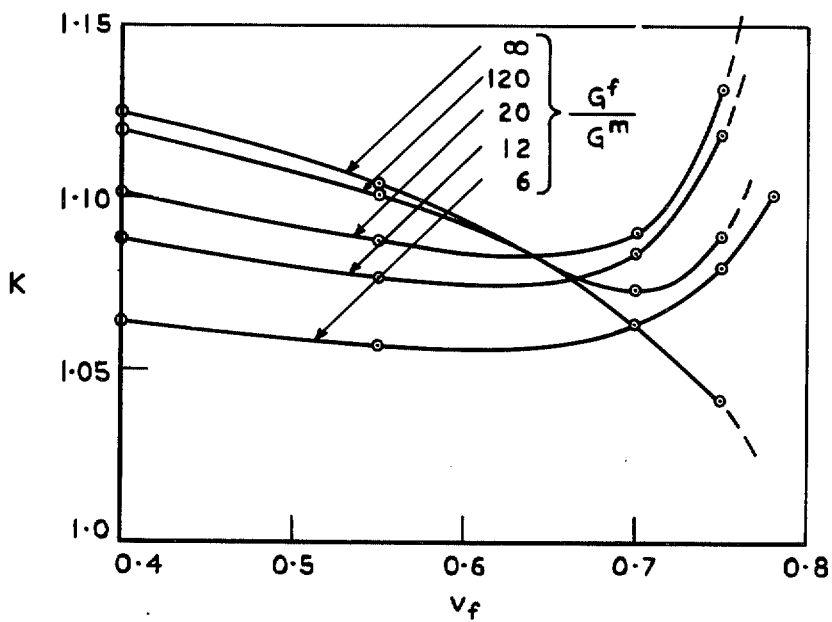


FIG. 6. Correction factors for square array

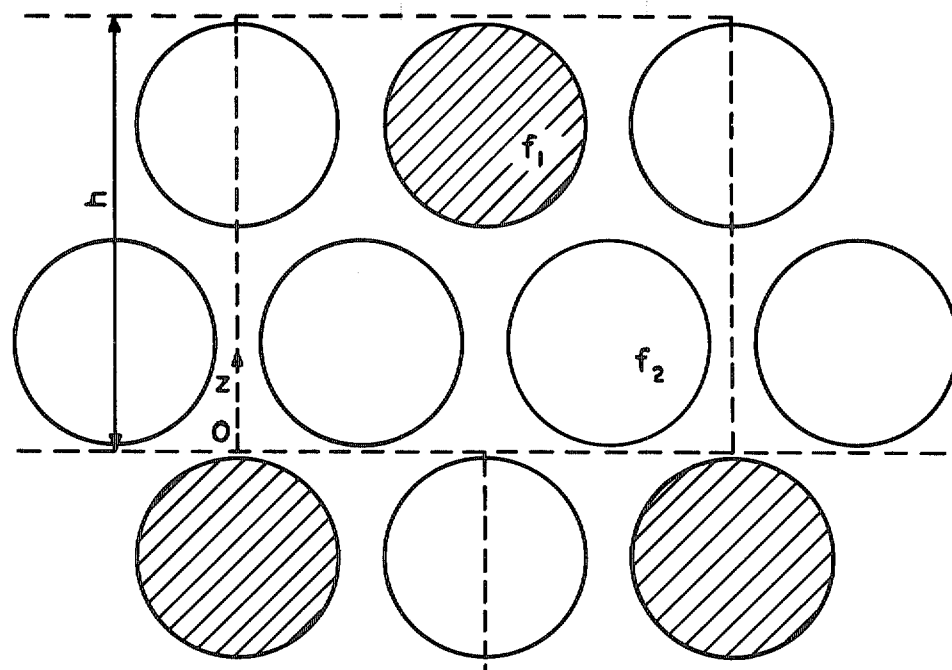


FIG. 7. Fibres with differing moduli in hexagonal array

R. & M. No. 3782

© Crown copyright 1976

HER MAJESTY'S STATIONERY OFFICE

Government Bookshops

49 High Holborn, London WC1V 6HB
13a Castle Street, Edinburgh EH2 3AR
41 The Hayes, Cardiff CF1 1JW
Brazennose Street, Manchester M60 8AS
Southey House, Wine Street, Bristol BS1 2BQ
258 Broad Street, Birmingham B1 2HE
80 Chichester Street, Belfast BT1 4JY

*Government publications are also available
through booksellers*

R. & M. No. 3782
ISBN 0 11 470953 X